

Neural Network-based Constant Current Control of Dynamic Wireless Power Supply System for Electric Vehicles

Yong Tian, Yue Sun, Yugang Su, Zhihui Wang and Chunsen Tang
College of Automation, Chongqing University, Chongqing 400030, China

Abstract: In the dynamic wireless power supply system for electric vehicles, the output current is influenced by factors, including primary rail current, relative position between pick-up unit and track, capacity of battery packs. Negative effect of those factors may lead to unsteady output. Aimed at the question of accurately modeling and output control caused by higher-order switch nonlinear behavior and multi-disturbance factor. An output current-stabilizing control strategy based on back-propagation (BP) neural network is proposed, making heavy use of nonlinear function approximation character and powerful generalization capability for neural network. With this strategy, the system was robust enough to unknown disturbance and parameter variation and output current can keep constant unswervingly. Finally, simulation results show that this control strategy has obvious advantages both in overshoot and setting time over conventional PID control method.

Key words: Electric vehicles, dynamical wireless power supply, back-propagation neural network, constant current control

INTRODUCTION

With soaring need of wireless power transfer (Green and Boys, 1994; Boys and Green, 1995; Kurs *et al.*, 2007; Aristeidis *et al.*, 2008) and green cars (Bai *et al.*, 2005), electric vehicles and wireless dynamic power supply technique (Covic *et al.*, 2007; Madawala and Thrimawithana, 2010; Seungyoung and Joungcho, 2011) have become hot research areas in recent years. In the electric vehicle wireless dynamic power supply system, on the one hand, the relative move between power emission unit (primary part) and power pick-up unit (second part) leads to change of coupled parameter which results in output fluctuation; on the other hand, the nonlinear and higher order and characters of system which result from the existence of vast nonlinear switching and energy-storage devices, make it hard to build the accurate system model and control. Neural network (NN) is an algorithm that can deal with higher-order, nonlinear, strong-coupled, uncertain and complex matter very well (Abdalla and Deris, 2005; Edriss *et al.*, 2008; Reddy *et al.*, 2008; Mahi and Izabatene, 2011; Alsaade, 2011). With powerful ability in nonlinear mapped, it is good at self-learning and self-organizing (Venkatachalam *et al.*, 2008; Guo *et al.*, 2011). Under NN control, a higher-order, nonlinear and model hard to build system can be robust.

There are two ways to regulate output power, primary control and secondary control. Phase-shift control (Yugang *et al.*, 2008; Yue *et al.*, 2009), primary detuning control (Ping *et al.*, 2008) and primary power injecting control (Xin *et al.*, 2011) are the several common methods which ask to send second part output parameter to primary controller via added communication device such as infrared, radio frequency and so on. In the dynamic wireless power supply system for electric vehicles, obviously it is difficult to build an effective communication system between primary part and second part. In addition, the real-time transfer of signal cannot be insured. Therefore, for the dynamic wireless power supply system for electric vehicles, the latter one is more feasible. Some previous studies have proposed the principle of second part power regulate (Hu *et al.*, 2000; Sallan *et al.*, 2009) but an effective control strategy has not been given.

From the above analysis, a constant current control strategy based on BP neural network, used in electric vehicles dynamic wireless power supply is presented in this paper. Using the nonlinear function approximation ability of neural network keeps the output current constant via regulating the duty ratio of power control switch as the pickup and track become misaligned which leads to the coupling parameter change. Then, a simulation model is built in the Simulink to verify that this control strategy is much better than conventional PID control method both in overshoot and setting time.

DYNAMIC WIRELESS POWER SUPPLY SYSTEM FOR ELECTRIC VEHICLES

Principle: The wireless power supply system for electric vehicles mainly employs inductive coupling (Chaoui *et al.*, 2005; Hmida *et al.*, 2007), magnetic resonance and microwave, replacing wires and connectors to transmit electric energy from power supply to load. Figure 1 shows the fundamental structure of electric vehicle power supply system based on inductively coupled power transfer technique (EVPS-ICPT). Primary power converter takes power from a conventional single-phase or three-phase power supply to generate a high frequency current in the primary energy emission unit (underground track or coil array), around which high frequency magnetic field is formed. In the pick-up unit which is located in the high frequency magnetic field, high frequency current is induced and conditioned by the onboard converter and controller to produce stable supply to battery charging or motor driving.

Main circuit: Four basic resonant topologies of ICPT system labeled as SS, SP, PS and PP can be employed in the inductively coupled power transfer system (Green and Boys, 1994), where the first S or P stands for series or parallel compensation of the primary winding and the second S or P stands for series or parallel compensation of the secondary winding. Since the series-compensated secondary reflects no reactance at the nominal resonant frequency, the primary inductance can be tuned out independent of either the magnetic coupling or the load by a series-connected capacitance in the primary network. As the parallel-compensated secondary reflects a load-independent capacitive reactance at the nominal resonant frequency, series tuning in the primary is dependent on the magnetic coupling but not the load. Because the reflected impedance contains a real component representing the load, parallel tuning in the primary becomes dependent on both the magnetic coupling and the load. What's more, SS and SP compensation are more advantageous for high-power transmission. At low-power levels, where wire section is not a relevant parameter, PS and PP compensations make possible working at a larger distance with the same operating frequency. Theoretically, SS is the best topology, as the primary capacitance is then independent of either the magnetic coupling or the load and is viable for high-power transmission. Considering capacitor requirements, however, parallel compensation implies lower voltages and higher currents than series compensation and requires lower operating frequency. That is due to the fact that the higher the required current, the lower the

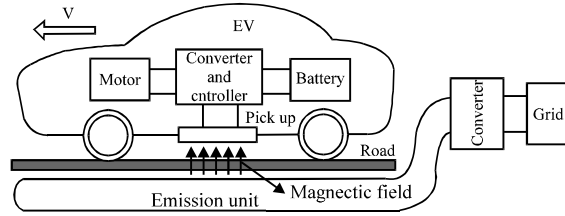


Fig. 1: Block diagram of system

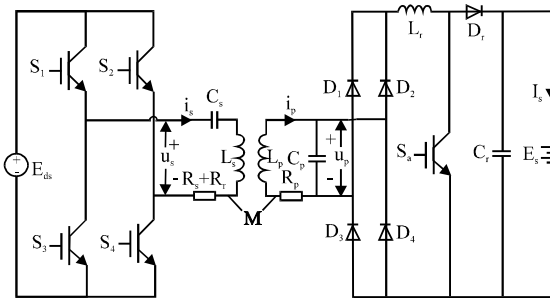


Fig. 2: Main circuit topology

operating frequency (Sallan *et al.*, 2009). Therefore, SP topology is also widely used for EVPS-ICPT application. A typical main circuit based on SP topology for EVPS-ICPT is shown in Fig. 2. It shows that the main circuit consists of power emission side (primary part) and pick-up part (second part) settled on car. The primary converter, composed of S_1 - S_4 , derives power from DC source E_{dc} and generates a track current in L_s which is loosely coupled to the pick-up winding L_p . The onboard rectifier, composed of D_1 - D_4 , converts induced high frequency ac current to dc current to battery pack charging. The power controller that consists of D_r , S_s and D_r can regulate the rank of charging power. C_s , R_s , R_r , C_p and R_p are the primary compensation capacitor, internal resistance of primary track, reflected resistance, secondary compensation capacitor and internal resistance of secondary pick-up winding respectively.

The mutual inductance between L_s and L_p is denoted as M , whose value is given by:

$$M = k\sqrt{L_s L_p} \tag{1}$$

where, k stands for the coupling coefficient between L_s and L_p .

To transfer maximum power to the load, the system should operate at the point of natural resonant frequency, whose value is determined by:

$$\omega = \frac{1}{\sqrt{L_p C_p}} \tag{2}$$

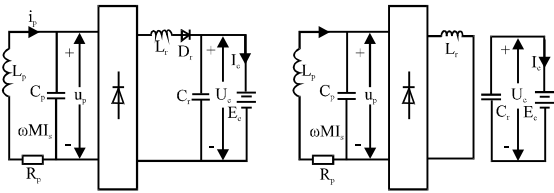


Fig. 3: Equivalent circuit as switch S_a on and off (a) S_a on (b) S_a off

where, C_p is the value of secondary compensation capacitor.

The value of primary compensation capacitor can be calculate by:

$$C_s = \frac{1}{\omega^2(L_s - M^2/L_p)} \quad (3)$$

The real part of reflected impedance is given by:

$$R_r = \text{Re}\left(\frac{\omega^2 M^2}{j\omega L_p + R_p + \frac{1}{j\omega C_p + 1/R_{eq}}}\right) \quad (4)$$

For maximum power transfer purpose, the dc inductance L_r is normally designed to be a value determined by Eq. 5 to ensure the continuation of the dc current I_c under the steady-state conditions:

$$L_r \geq R_{min}/\omega \quad (5)$$

where, R_{min} is the equivalent resistance of the maximum load.

Power regulating: Power control is finished by a Booster which consists of L_r , S_a and D_r . The equivalent circuit as S_a on and off are showed in Fig. 3a and b, respectively. Supposed t_{on} as the time of S_a on and t_{off} as the time of S_a off. Then the output power can be regulated by changing the ration of t_{on} and t_{off} .

THE ARCHITECTURE AND ALGORITHM OF THE BP NEURAL NETWORK

The BP neural network is one of the most typical neural network models. It is very good at nonlinear fitting, prediction, generalization and error tolerance (Mullai and Rene, 2008; Yedjour *et al.*, 2011). A BP neural network has a layered structure (a single input layer, a single hidden layer or multi hidden layers, a single output layer). Each layer consists of units (neurons or nodes) which receive their input from units from a layer directly above and send their output to units in a layer directly below the unit. There are no connections among units in the same layer.

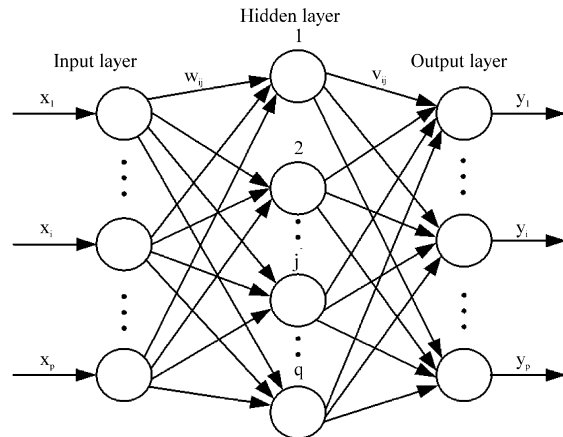


Fig. 4: Block diagram of three-layered BP neural network

A tri-layer BP neural network, whose number of neurons of input layer, hidden layer and output layer are p , q and r , respectively, is shown in Fig. 4.

Mark $X = [x_1, x_2, \dots, x_p]$ as the input vector, $Y = [y_1, y_2, \dots, y_q]$ as the output vector, w_{ij} ($i = 1, 2, \dots, p$; $j = 1, 2, \dots, q$) as the weight between the input layer node i and hidden layer node j , v_{jt} ($j = 1, 2, \dots, q$; $t = 1, 2, \dots, r$) as the weight between the hidden layer node j and output layer node t , θ_j as the threshold of hidden layer node j and γ_t as the threshold of output layer node t . Then:

$$S_j = \sum_{i=1}^p w_{ij} x_i - \theta_j \quad (6)$$

$$b_j = f(S_j) \quad (7)$$

$$L_t = \sum_{j=1}^q v_{jt} b_j - \gamma_t \quad (8)$$

$$y_t = g(L_t) \quad (9)$$

where, S_j , b_j , $f()$, L_t , y_t and $g()$ are the input of hidden node j , the output of hidden node j , the active function of hidden layer, the input of output layer node t , the output of output layer t and the active function of output layer, respectively.

Mark $e(k)$ as the error between actual and expected output and it is given by:

$$e(k) = y_o(k) - y_t(k) \quad (10)$$

The expression for energy function is:

$$E = \frac{1}{2} e(k)^2 \quad (11)$$

The BP neural network is a kind of learning algorithm for error correction built on the basis of gradient descent method which organically combined positive spread of

the input signal with back-propagation of error ones (Mianli *et al.*, 2010). While learning the new sample, it tends to forget the old ones, that is to say, it fails to take into account the previous experience. As a result, the local minimum problem and slow convergence speed will exist. To solve these issues, three major methods have been introduced:

- Change the learning efficiency
- Add momentum factor
- Appropriate transfer function

Method 1 and 2 are adopted in this paper. Thus, we can get the following expressions:

$$\Delta w_{ij} = -\eta \frac{\partial E}{\partial w_{ij}} = -\eta \cdot e(k) \cdot \frac{\partial y_i}{\partial w_{ij}} \quad (12)$$

$$\Delta v_{jt} = -\eta \frac{\partial E}{\partial v_{jt}} = -\eta \cdot e(k) \cdot \frac{\partial y_i}{\partial v_{jt}} \quad (13)$$

$$w_{ij}(k+1) = w_{ij}(k) + \Delta w_{ij} + \alpha(w_{ij}(k) - w_{ij}(k-1)) \quad (14)$$

$$v_{jt}(k+1) = v_{jt}(k) + \Delta v_{jt} + \alpha(v_{jt}(k) - v_{jt}(k-1)) \quad (15)$$

where, $\eta \in [0,1]$ and $\alpha \in [0,1]$ stands for learning efficiency and momentum factor, respectively.

DESIGN OF THE BP NEURAL NETWORK CONTROLLER

In this study, we use a 3-q-2 BP neural model, whose number of input layer nodes, hidden layer nodes and output layer nodes are 3, q and 2. The error e between actual output current and reference current, reference current I_{ref} and mutual inductance are the three nodes of input layer. The duty ratio variation Δd of switch S_a and reference duty ration d_0 are the two node of output layer. The number of hidden layer nodes has a huge effect on the ability in function approximation of BP neural network but more hidden layer nodes is not always better. Usually long learning time, bad error tolerance and failed to identify new sample all result from too many hidden layer nodes. An optimized number of hidden layer is given by the following empirical equation:

$$q = \sqrt{p+r} + a, \quad a \in [1,10] \quad (16)$$

where, q is the number of hidden layer nodes, p is the number of input layer nodes and r is the number of output layer nodes.

Based on Eq. 16, 10 hidden layer nodes is suitable. And then, a simulation model is built and its primary configuration parameters as following:

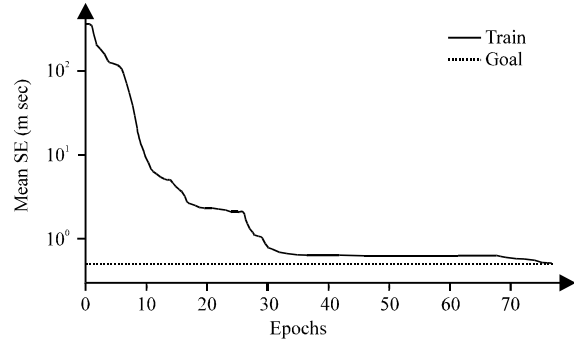


Fig. 5: The mean square error function curve of simulation model

Table 1: Partial training data

I_{ref}/A	e/A	$M/\mu H$	d_0 (%)	Δd (%)
6	-0.279	2.0	28	-22
6	-0.24	2.0	28	-12
6	-0.038	2.0	28	-2
6	0.093	2.0	28	3
6	0.238	2.0	28	8
6	0.543	2.0	28	18
6	-0.633	2.2	18	-32
6	-0.581	2.2	18	-22
6	-0.361	2.2	18	-12
6	-0.063	2.2	18	-2
6	0.098	2.2	18	3
6	0.261	2.2	18	8
6	0.424	2.2	18	13
6	-0.818	2.4	9	-26
6	-0.53	2.4	9	-16
6	-0.352	2.4	9	-11
6	-0.088	2.4	9	-3
6	-0.019	2.4	9	-1
6	0.049	2.4	9	1
6	0.153	2.4	9	4
6	0.254	2.4	9	7
6	-1.349	2.6	2	-48
6	-1.265	2.6	2	-38
6	-1.004	2.6	2	-28
6	-0.663	2.6	2	-18
6	-0.298	2.6	2	-8
6	-0.116	2.6	2	-3

- The active function of input layer to hidden layer: double tangent S function “tansig”
- The active function of hidden layer to output layer: linear function “purelin”
- The train function: reflected propagation algorithm “trainlm”
- Weights correct rule: momentum gradient descent learning function “learnrnm”
- Learning speed: 0.05
- Maximum train steep: 1000
- Target error: 0.05
- The train sample: includes data when mutual inductance is 2.0, 2.2, 2.4 and 2.6 μH . Partial training data is shown in Table 1

With the above parameters, the mean square error function curve is shown in Fig. 5.

It can be seen from Fig. 5 that the work meets the need of aim error after 77 iterations. This indicates that the system is able to converge with a high speed.

SIMULATIONS

In this section, a simulation model whose parameters are shown in Table 2 is built in the MATLAB/Simulink environment to verify the validity of BP neural network control method used in the dynamic wireless power supply system for electric vehicles.

Table 2: Parameters of the simulation model

Parameter	Value
Resonant capacitor $C_S = C_P$	2 μF
Resonant inductance $L_S = L_P$	31 μH
Equivalent load R_L	50 Ω
Operating frequency f_g	20 kHz
Input Voltage E_d	300 V

Figure 6 shows the control block diagram. The error e between referenced current and out current, the referenced current I_{ref} and the mutual inductance M are inputted in the BPNN controller which will give out the duty ratio variation Δd of switch S_a and reference duty ratio d_0 . The duty ratio d is calculated out by d calculator and used to drive the control circuit.

Figure 7, where, BPNN control is added at 0.02 sec and mutual inductance varies instantaneously from 2.4 to 2.0 μH at 0.08 sec and goes back 2.4 μH at 0.14 sec, demonstrates the control results of BP neural network control. To show the advantages of BP neural network control, the results of conventional PID method are shown in Fig. 8.

Figure 7 and 8 tell us that the regulate time of BPNN control method is only about 0.005 sec and the overshoot is less than 0.1 A. Contrastively, the overshoot of PID

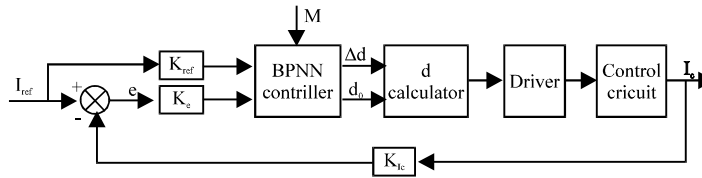


Fig. 6: Control block diagram of system

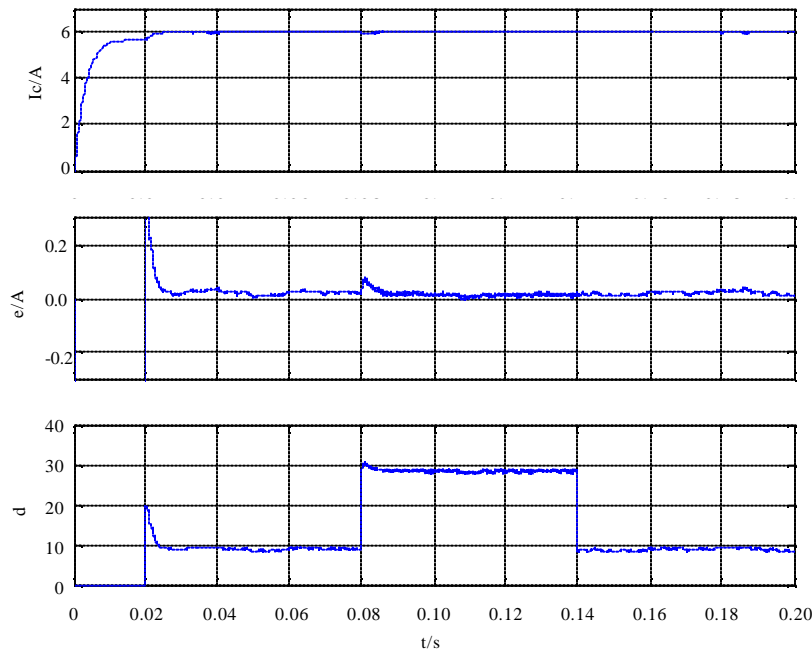


Fig. 7: Waveforms of BP neural network control method ($M = 2.0, 2.4 \mu\text{H}$)

control method is about -0.24 A ($\delta \approx 5\%$) and the regulate time is about 0.03 sec when the mutual inductance goes from 2.0 to 2.4 μH . And the overshoot is about 0.3 A ($\delta \approx 6.5\%$) and the regulate time is also about 0.03 sec when the mutual inductance goes back 2.0 μH .

Figure 9 shows this situation: mutual inductance varies instantaneously from 2.5 to 2.1 μH at 0.08 sec and goes back 2.5 μH at 0.14 sec. It verifies that the effect of BPNN control is also very good despite the input parameter is out of the training sample.

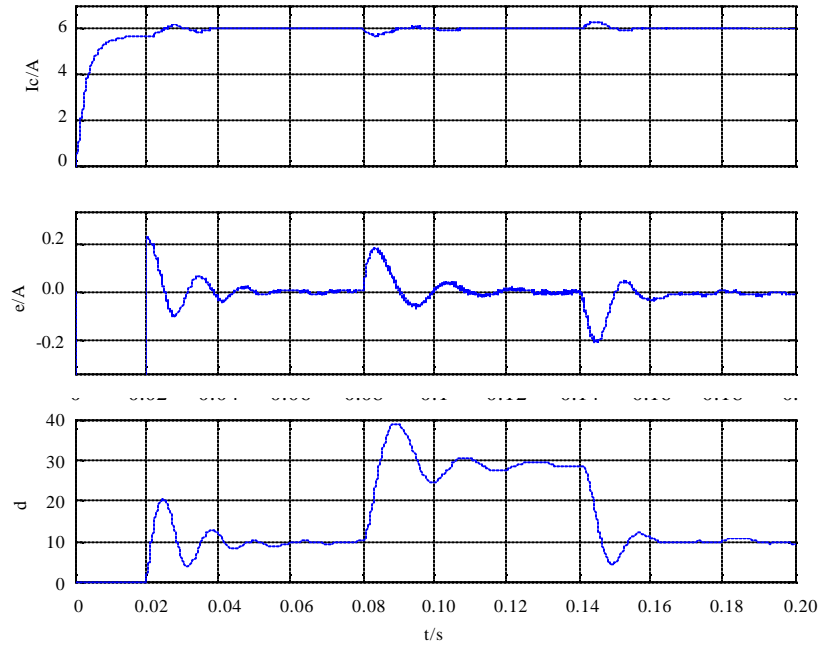


Fig. 8: Waveforms of PID control method ($M = 2.0, 2.4 \mu\text{H}$)

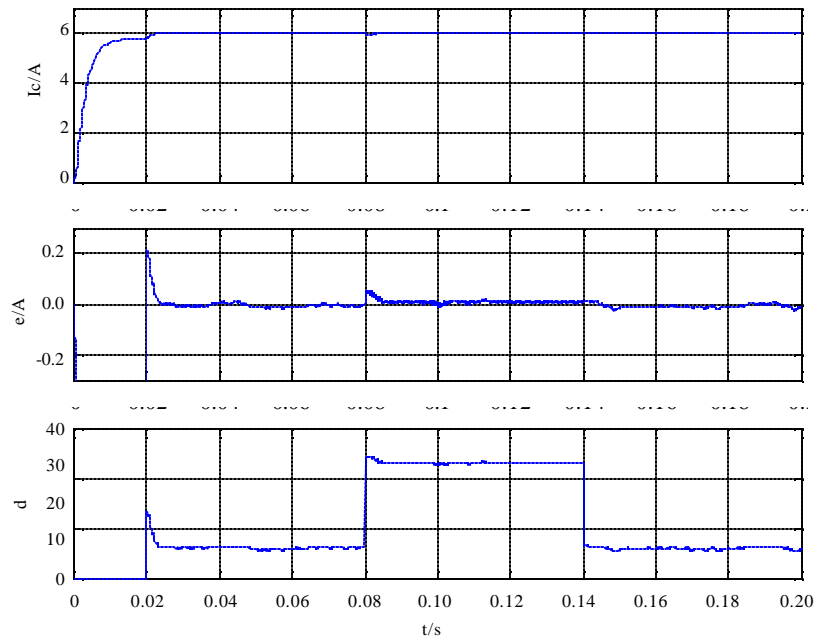


Fig. 9: Waveforms of BP neural network control method ($M = 2.1, 2.5 \mu\text{H}$)

CONCLUSIONS

In this study, a constant current control method based on the back-propagation neural network is proposed to solve the problem of wireless constant current charging for moving electric vehicles. Simulation results prove this method to be plausible, even when the input parameter is not in the training sample. By introducing this control method, the problem of accurately modeling and output control caused by higher-order nonlinear behavior and multi-disturbance factor can be satisfactorily resolved.

ACKNOWLEDGMENTS

This study is supported by the National Natural Science Foundation of China (No. 50807057) and the central university basic scientific research business project of China (No. CDJXS11172238).

REFERENCES

- Abdalla, S.O. and S. Deris, 2005. Predicting protein secondary structure using artificial neural networks: Current status and future directions. *Inform. Technol. J.*, 4: 189-196.
- Alsaade, F., 2011. An enhanced classification and prediction of neoplasm using neural network. *Asian J. Applied Sci.*, 4: 618-629.
- Aristeidis, K., J.D. Joannopoulos and S. Marin, 2008. Efficient wireless non-radiative mid-range energy transfer. *Ann. Phys.*, 323: 34-48.
- Bai, Z.F., S.X. Li and B.G. Cao, 2005. H_2 control applied to electric torque control for regenerative braking of an electric vehicle. *J. Applied Sci.*, 5: 1103-1107.
- Boys, J.T. and A.W. Green, 1995. Inductively coupled power transmission concept-design and application. *IPENZ Trans.*, 22: 1-9.
- Chaoui, M., H. Ghariani, M. Lahiani and F. Sellami, 2005. An optimal geometry for power energy and data transmission in the inductive link. *J. Applied Sci.*, 5: 1504-1513.
- Covic, G.A. J.T. Boys, M.L.G. Kissin and H.G. Lu, 2007. A three-phase inductive power transfer system for roadway-powered vehicles. *IEEE Trans. Ind. Elec.*, 54: 3370-3378.
- Edriss, M.A., P. Hosseinnia, M. Edrisi, H.R. Rahmani and M.A. Nilforooshan, 2008. Prediction of second parity milk performance of dairy cows from first parity information using artificial neural network and multiple linear regression methods. *Asian J. Anim. Vet. Adv.*, 3: 222-229.
- Green, A.W. and J.T. Boys, 1994. 10 kHz inductively coupled power transfer concept and control. *Proceedings of the 5th International Conference on Power Electronics and Variable Speed Drivers*, October 26-28, 1994, London, pp: 694-699.
- Guo, L., B. Wang, W. Wang, Z. Liu and C. Gao, 2011. Energy function analysis and optimized computation based on hopfield neural network for wireless sensor network. *Inform. Technol. J.*, 10: 1208-1214.
- Hmida, G.B., H. Ghariani and M. Samet, 2007. Design of wireless power and data transmission circuits for implantable biomicrosystem. *Biotechnology*, 6: 153-164.
- Hu, A.P., J.T. Boys and G.A. Covic, 2000. Frequency analysis and computation of a current-fed resonant converter for ICPT power supplies. *Proceedings of the International Conference on Power System Technology*, December, 2000 Dept. of Electr. and Electron. Eng., Auckland Univ., Australia 327-332.
- Kurs, A., A. Karalis, R. Moffatt, J.D. Joannopoulos, P. Fisher and M. Soljacic, 2007. Wireless power transfer via strongly coupled magnetic resonances. *Science* 317: 83-86.
- Madawala, U.K. and D.J. Thrimawithana, 2010. A ring inductive power transfer system. *Proceeding of the International Conference on Industrial Technology*, March 14-17, 2010 Dept. of Electr. and Comput. Eng., Univ. of Auckland, Auckland, New Zealand, Chile 667-672.
- Mahi, H. and H.F. Izabatene, 2011. Segmentation of satellite imagery using RBF neural network and genetic algorithm. *Asian J. Applied Sci.*, 4: 186-194.
- Mianli, W., L. Jie, X. Xin and Z. Zhong, 2010. Improvement of sampling precision in Li-ion battery formation system by using BP neural network. *J. Cen. South Univ. Sci. Technol.*, 41: 55-59.
- Mullai, P. and E.R. Rene, 2008. A simple multi layered neural network model for predicting bacterial xylanase production by *Bacillus* sp. Using *Avena sativa* as substrate. *Biotechnology*, 7: 499-504.
- Ping, S., A.P. Hu, S. Malpas and D. Budgett, 2008. A frequency control method for regulating wireless power to implantable devices. *IEEE Trans. Biomed. Cir. Sys.*, 2: 22-29.
- Reddy, B.S., G. Padmanabhan and K.V.K. Reddy, 2008. Surface roughness prediction techniques for CNC turning. *Asian J. Sci. Res.*, 1: 256-264.
- Sallan, J., J.L. Villa, A. Llombart and J.F. Sanz, 2009. Optimal design of ICPT systems applied to electric vehicle battery charge. *IEEE Trans. Ind. Elec.*, 56: 2140-2149.

- Seungyoung, A. and K. Joung, 2011. Magnetic field design for high efficient and low EMF wireless power transfer in on-line electric vehicle. Proceedings of the 5th European Conference on Antennas and Propagation, April 11-15, 2011 Dept. of EECS, Korea Adv. Inst. of Sci. and Technol., Daejeon, South Korea, Italy 3979-3982.
- Venkatachalam, S., C. Arumugam, K. Raja and V. Selladurai, 2008. Quality function deployment in agile parallel machine scheduling through neural network technique. *Asian J. Scientific Res.*, 1: 146-152.
- Xin, D., Y. Sun and Y. Su, 2011. Study on constant current control of inductive power transfer with parameter identification. *J. Chon. Univ.*, 34: 98-104.
- Yedjour, D., H. Yedjour and A. Benyettou, 2011. Combining quine mc-cluskey and genetic algorithms for extracting rules from trained neural networks. *Asian J. Applied Sci.*, 4: 72-80.
- Yue, S., W. Zhi-hui and S. Yugang, 2009. Power transfer regulation mode for current fed CPT system. *J. Chon. Univ.*, 32: 1386-1391.
- Yugang, S., W. Zhihui, Y. Sun and T. Chunsen, 2008. Modeling of contactless power transfer systems with a phase-shifted control method. *Trans. China Elec. Soc.*, 23: 92-97.